



Enhanced light output of CsI(Na) scintillators by photonic crystals

Xiao Ouyang ^{a,b,*}, Bo Liu ^d, Xincheng Xiang ^{a,b}, Liang Chen ^c, Mengxuan Xu ^c, Xiaojing Song ^c, Jinlu Ruan ^c, Jinliang Liu ^c, Chuanxiang Chen ^d, Zhichao Zhu ^d, Yang Li ^e

^a Institute of Nuclear and New Energy Technology, Tsinghua University, Beijing, 100084, China

^b Beijing Key Laboratory of Nuclear Detection, Beijing, 100084, China

^c State Key Laboratory of Intense Pulsed Radiation Simulation and Effect, Northwest Institute of Nuclear Technology, Xi'an, Shanxi 710024, China

^d School of Physics Science and Engineering, Tongji University, Shanghai 200092, China

^e Department of Nuclear Science and Engineering, Nanjing University of Aeronautics and Astronautics, Nanjing 211106, China



ARTICLE INFO

Keywords:

CsI(Na) scintillator

Photonic crystal

Light output enhancement

ABSTRACT

We have demonstrated that the scintillation light output of CsI(Na) crystals can be enhanced by photonic crystals consisting of arrays of nanospheres. The photonic crystals on the surfaces of the CsI(Na) crystals were prepared by a dry-transfer technology which is a suitable method for hygroscopic scintillators. Under the excitation of X-ray, compared with a reference sample, a 2.79-fold wavelength-integrated enhancement has been obtained for the optimal photonic crystal parameters. The increased light output could improve the performance of scintillator-based detectors.

1. Introduction

CsI(Na) crystals have unique physical properties, such as relatively high density (4.53 g/cm³), high scintillation light yield (38,500 ph./MeV), good plasticity, and excellent irradiation resistance [1–3]. Thus CsI(Na) crystals are ideal scintillation materials which can be widely applied to different domains, such as nuclear radiation detection, high-energy physics experiments, detection of dark matter, nuclear medical imaging and space exploration [4–11]. Recently, it is reported that a fast decay component of CsI(Na) crystals could be dominant when their grain diameters decrease to micron-scale [12–14].

Scintillators with high refractive indices often suffer from a poor light extraction efficiency because the scintillation light with an incident angle larger than the critical angle will be trapped inside the crystals due to total internal reflection (TIR), and thus cannot reach the photodetectors, such as photomultiplier tubes and photodiodes. For example, CsI(Na) has a refractive index of 1.8. The extraction efficiency from one side of the crystal-air interface is as low as 7.7% according to an approximate formula ($1/4 n^2$) [15].

Photonic crystals (PhCs) have been used to improve the extraction efficiency through the coupling of the evanescent field and the periodic structures of PhCs [16–19]. The preparation methods of PhCs on the surfaces of scintillators include self-assembly, interference lithography, hot embossing and electron beam lithography [19–24].

In this paper, we demonstrate an enhanced light output for CsI(Na) scintillators by using PhCs prepared with a dry-transfer technology. The scintillation time profiles and the emission spectra of the samples are characterized. The enhancement mechanism is discussed in detail.

2. Methods of experiments and numerical simulations

CsI(Na) single-crystal samples used in the experiments have a dimension of $\Phi 30$ mm \times 2 mm. PhCs in the present investigation are composed of hexagonal close-packed arrays of polystyrene (PS) nanospheres with selected diameters of 300, 400, 500 and 600 nm. The PhCs were coated onto the surfaces of the CsI(Na) samples by a dry-transfer technique which is a suitable method for hygroscopic scintillators. The arrays of nanospheres prefabricated on the surfaces of silicon wafers were dry-transferred to the surfaces of the CsI(Na) samples in order to avoid touching water. Finally, a conformal layer of titanium oxide (refractive index $n = 2.6$) with a thickness of 30 nm was deposited on the array of nanospheres by atomic layer deposition (ALD) technology to increase the refractive index contrast [25].

Fig. 1 shows the experimental setup for the measurement of the scintillation time profiles excited by pulsed X-ray. Pulsed electron beams with an energy of 30 MeV generated in an accelerating tube were used to produce pulsed X-ray. The frequency of excitation pulses is set to be 10 Hz. The scintillation light from the samples without wavelength-resolution was collected by a photomultiplier tube (ETL9850B, U.K.). The waveforms of the output signals were recorded by an oscilloscope (DPO70604C).

The emission spectra were measured with a portable X-ray source manufactured by Moxtek Inc. The X-ray source was operated under the voltage of 30 kV and the current of 250 μ A. A spectrometer (Newport 74216) and a photomultiplier tube (Newport77360) were used to record

* Corresponding author at: Institute of Nuclear and New Energy Technology, Tsinghua University, Beijing, 100084, China.

E-mail address: oyx16@mails.tsinghua.edu.cn (X. Ouyang).

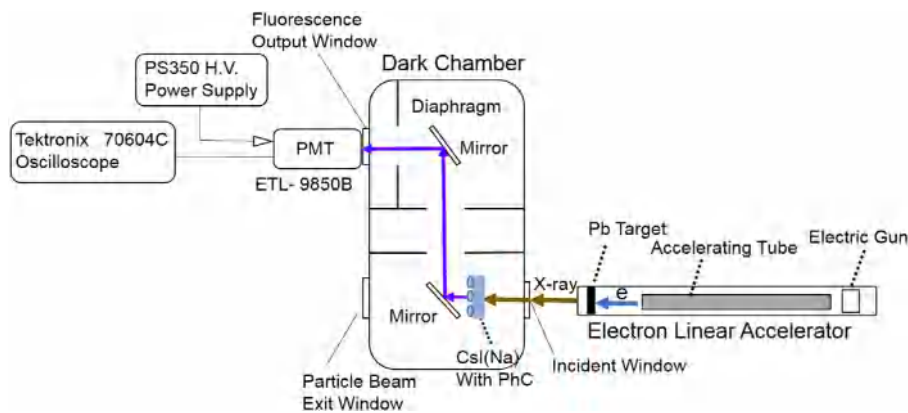


Fig. 1. Experimental setup for the measurement of scintillation time profiles excited by pulsed X-ray.

the emission spectra of the samples. The photomultiplier tube was operated under the working voltage of -800 V. The samples fixed at 1.5 cm away from the slit with a width of 1 mm of the monochromator were excited by the X-ray source placed 13.5 cm away from the samples.

The numerical simulations for the transmission spectra with different polarizations were performed based on a rigorous coupled wave analysis (RCWA) method. Periodic boundary conditions were used.

3. Results and discussion

The simulated transmission spectra for s-polarization, p-polarization as a function of incident angle at the wavelength of 420 nm for the CsI(Na) samples coated with PhCs and a reference sample without a PhC are shown in Fig. 2.

For the reference sample, the transmission drops to zero beyond the critical angle of 33.7° . For the samples coated with PhCs, several extra transmission peaks appear for both s-polarization and p-polarization beyond the critical angle, which implies that some scintillation light trapped inside the crystals as a result of TIR could be out coupled by the PhCs, leading to an enhanced extraction efficiency. These peaks belong to the whispering gallery modes due to the Mie resonance of individual nanospheres and the Bragg diffraction arising from the periodic arrangements [26]. The evanescent field near the interface can be coupled into the arrays of nanospheres, which can be further coupled into the air by the periodic arrangements [21]. The angles of these peaks are strongly dependent on the period of PhCs (the diameters of nanospheres for a hexagonal close-packed array). Different periods also exhibit different diffraction efficiencies. In addition, it is found that several transmission dips appear below the critical angle, which results in some extra diffraction back into the crystals. However, the back-diffracted light can be re-extracted by the PhCs, which enables an enhanced ultimate extraction efficiency.

Fig. 3(a) shows the X-ray excited emission spectra with a broad band peaking at about 420 nm which is attributed to a typical emission band from the Na-related exciton of CsI(Na) crystals [27–29]. The emission intensity of the samples coated with PhCs is significantly enhanced in the entire spectral range. Fig. 3(b) shows the enhancement ratio with respect to the reference sample. The sample with the PhC (diameter of nanospheres $D = 400$ nm) exhibits the maximum enhancement ratio. One can find two obvious enhancement bands peaking at 440 nm and 630 nm. The spectrally-integrated enhancement ratio reaches 2.79 . The PhCs with different diameters (D values) give rise to different enhancement ratios which are highly wavelength-dependent. Such wavelength-dependence is the inherent characteristic of diffraction due to the periodic structures of PhCs [21].

Figs. 4(a) and 4(b) present the X-ray excited decay time profiles of the CsI(Na) samples coated with PhCs and the reference sample for both voltage amplitude and normalized amplitude, respectively. All of

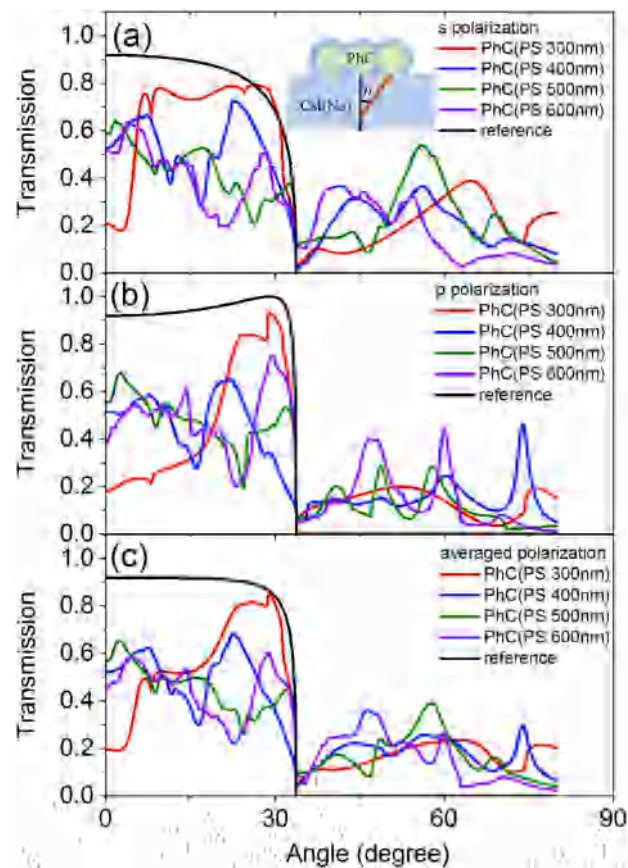


Fig. 2. Simulated transmission spectra for s-polarization (a), p-polarization (b) and their averages (c) as a function of incident angle at the wavelength of 420 nm for the CsI(Na) samples coated with PhCs and a reference sample.

the decay time profiles are well fitted with a double-exponential decay function according to the Eq. (1).

$$I(t) = I_0 + A_1 e^{-(t-t_0)/\tau_1} + A_2 e^{-(t-t_0)/\tau_2} \quad (1)$$

Where, I_0 is the background signal, t_0 is the starting point of decay time, A_1 and A_2 are the amplitudes, τ_1 and τ_2 are the decay time constants.

The fitting parameters are shown in Table 1. For the reference sample, the decay time constants are 572 ns and 3019 ns. The former is the typical decay characteristic of the Na-related exciton emission in CsI(Na) [30]. The latter is a slow component, possibly due to some deep traps in the crystals. It is found that the decay time constants of

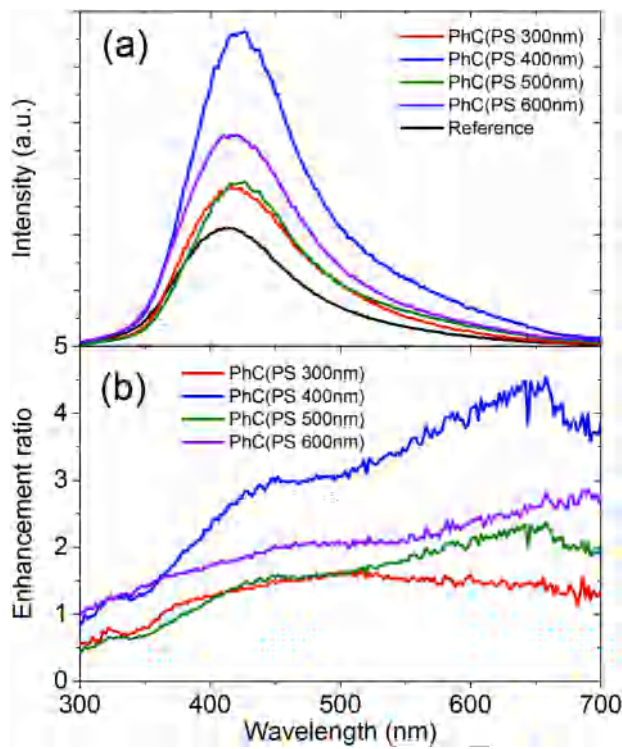


Fig. 3. X-ray excited emission spectra (a) and the enhancement ratio (b) for the CsI(Na) samples coated with PhCs.

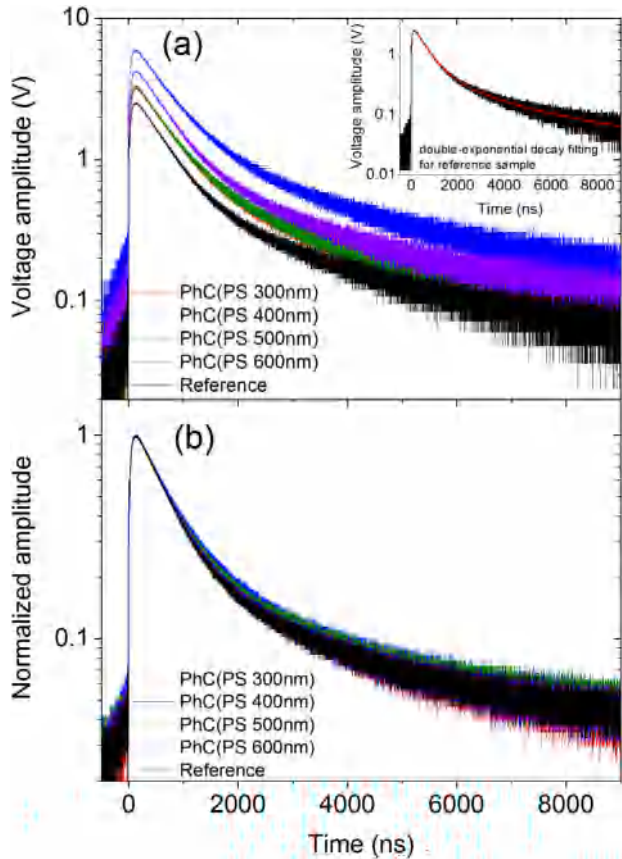


Fig. 4. X-ray excited scintillation time profiles of the CsI(Na) samples coated with PhCs and the reference sample for the voltage amplitude (a) and the normalized amplitude (b). The inset in (a) is a double-exponential decay fitting for the reference sample.

Table 1

Fitting parameters of the scintillation decay time profiles.

CsI(Na) samples	τ_1/ns	τ_2/ns	A_1/A_2	I_0 (V)
Reference	572	3019	4.05	0.04
PhC ($D = 300 \text{ nm}$)	612	3090	3.66	0.06
PhC ($D = 400 \text{ nm}$)	620	2984	3.17	0.11
PhC ($D = 500 \text{ nm}$)	606	2949	3.53	0.06
PhC ($D = 600 \text{ nm}$)	577	3014	3.81	0.07

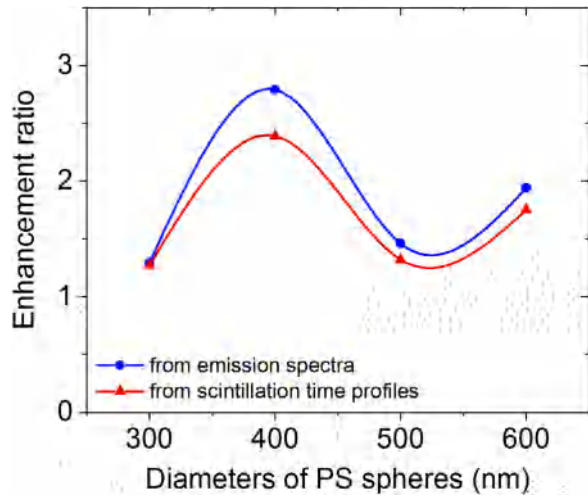


Fig. 5. Spectrally-integrated enhancement ratio by PhCs with different diameters from the measurements of the emission spectra and the scintillation time profiles.

the Na-related exciton emission increase for the CsI(Na) samples coated with PhCs. The longest decay time constant is 620 ns for the PhC with $D = 400 \text{ nm}$. While, the decay time constants of the slow component have a slight decrease, except for the case of PhC with $D = 300 \text{ nm}$. The different changing trends suggest that the variation of the time constants seems unlikely to be related with the PhCs. It is perhaps due to the difference of the scintillators themselves. The background signal I_0 increases for the CsI(Na) samples coated with PhCs, which is probably due to a pile-up effect at the excitation frequency of 10 Hz. Despite a low frequency of excitation pulses of 10 Hz applied, a longer lasting afterglow component may exist, forming the background signal which can also been enhanced by the PhCs.

The decay time profiles for the voltage amplitude shown in Fig. 4(a) also provide the intensity information, which can be used to calculate the light output enhancement ratios since the samples were measured under identical conditions. The enhancement ratios as a function of diameter of nanospheres from the measurements of the decay time profiles and the emission spectra are plotted in Fig. 5. These two measurements show basically consistent results with the optimal PhC parameter of diameter ($D = 400 \text{ nm}$). The slight divergences of the enhancement ratios could be attributed to the different spectral responses of the photomultiplier tubes and the spectrometers.

4. Conclusion

The scintillation light output of CsI(Na) crystals can be significantly enhanced by the PhCs which consist of arrays of nanospheres. A dry-transfer technology was used to prepare the PhCs on the surfaces of CsI(Na) crystals due to their hygroscopic characteristics. For the optimal PhC parameter, a 2.79-fold enhancement was achieved. Such enhanced light output of CsI(Na) crystals is advantageous to the practical applications especially under the situations of weak signal detections.

CRediT authorship contribution statement

Xiao Ouyang: Conceptualization, Investigation, Writing - original draft. **Bo Liu:** Methodology, Writing - review & editing. **Xincheng Xiang:** Supervision, Project administration, Funding acquisition. **Liang Chen:** Investigation. **Mengxuan Xu:** Investigation. **Xiaojing Song:** Investigation. **Jinlu Ruan:** Investigation. **Jinliang Liu:** Investigation. **Chuanxiang Chen:** Investigation. **Zhichao Zhu:** Software, Formal analysis, Data curation. **Yang Li:** Investigation.

Declaration of competing interest

The authors declare that they have no known competing financial interests or personal relationships that could have appeared to influence the work reported in this paper.

Acknowledgments

This work is supported by the National Natural Science Foundation of China (Grant Nos. 11435010 and 11975168).

References

- [1] K. Imanaka, A.H. Kayal, A. Mezger, J. Rossel, Self-trapped exciton luminescence after tunnelling of V_K and Na centers in $CsI: Na$ crystals, *Phys. Status Solidi B* 108 (1981) 449–458.
- [2] V. Yakovlev, L. Trefilova, A. Meleshko, Y. Ganja, Short-living absorption and emission of $CsI (Na)$, *J. Lumin.* 131 (2011) 2579–2581.
- [3] E. Khodadoost, M.A. Araghi, Scintillation response of Europium and Indium-co-doped $CsI (Na)$ single crystal under the exposure of gamma-ray, *Nucl. Instrum. Methods Phys. Res. A* 942 (2019) 162351.
- [4] J. Collar, N. Fields, M. Hai, T. Hossbach, J. Orrell, C. Overman, G. Perumpilly, B. Scholz, Coherent neutrino-nucleus scattering detection with a $CsI [Na]$ scintillator at the SNS spallation source, *Nucl. Instrum. Methods Phys. Res. A* 773 (2015) 56–65.
- [5] J. Collar, A. Kavner, C. Lewis, Response of $CsI [Na]$ to nuclear recoils: Impact on coherent elastic neutrino-nucleus scattering, *Phys. Rev. D* 100 (2019) 033003.
- [6] N. Giokaris, G. Loudos, D. Maintas, A. Karababounis, M. Lembesi, V. Spanoudaki, E. Stiliaris, S. Boukis, N. Sakellios, N. Karakatsanis, Comparison of $CsI (Tl)$ and $CsI (Na)$ partially slotted crystals for high-resolution SPECT imaging, *Nucl. Instrum. Methods Phys. Res. A* 569 (2006) 185–187.
- [7] I. Kilimchuk, V. Gavril'yuk, B. Grinyov, V. Tarasov, Y.T. Viday, Features of scintillation characteristics of $CsI: Na$ and $NaI: Tl$ crystals as the basis for soft gamma radiation detectors, *Opt. Mater.* 30 (2008) 1800–1802.
- [8] W. Lee, T. Lee, A compact Compton camera using scintillators for the investigation of nuclear materials, *Nucl. Instrum. Methods Phys. Res. A* 624 (2010) 118–124.
- [9] W. Mengesha, T. Taulbee, B. Rooney, J. Valentine, Light yield nonproportionality of $CsI (Tl)$, $CsI (Na)$, and YAP, *IEEE Trans. Nucl. Sci.* 45 (1998) 456–461.
- [10] X. Sun, J. Lu, T. Hu, L. Zhou, J. Cao, Y. Wang, L. Zhan, B. Yu, X. Cai, J. Fang, Neutron-gamma discrimination of $CsI (Na)$ crystals for dark matter searches, *Nucl. Instrum. Methods Phys. Res. A* 642 (2011) 52–58.
- [11] A. Syntfeld-Kazuch, P. Sibczyński, M. Moszyński, A. Gektin, W. Czarnacki, M. Grodzicka, J. Iwanowska, M. Szawłowski, T. Szczęśniak, Energy resolution of $CsI (Na)$ scintillators, *Radiat. Meas.* 45 (2010) 377–379.
- [12] X. Ouyang, B. Liu, X. Xiang, L. Chen, M. Xu, X. Song, J. Ruan, L. Liu, J. Liu, C. Chen, $CsI (Na)$ micron-scale particles-based composite material for fast pulsed X-ray detection, *Nucl. Instrum. Methods Phys. Res. A* 953 (2020) 163120.
- [13] F. Liu, X. Ouyang, B. Liu, J. Liu, L. Chen, Z. Zhang, X. Zhang, Y. Feng, Size-induced effect on cathode luminescence spectra of $CsI (Na)$ and $CsI (Tl)$ crystals, *Sci. China A* 57 (2014) 1684–1688.
- [14] F. Liu, X. Ouyang, M. Tang, Y. Xiao, B. Liu, X. Zhang, Y. Feng, J. Zhang, J. Liu, Scaling-induced enhancement of X-ray luminescence in $CsI (Na)$ crystals, *Appl. Phys. Lett.* 102 (2013) 181107.
- [15] K. McGroddy, A. David, E. Matioli, M. Iza, S. Nakamura, S. DenBaars, J. Speck, C. Weisbuch, E. Hu, Directional emission control and increased light extraction in GaN photonic crystal light emitting diodes, *Appl. Phys. Lett.* 93 (2008) 103502.
- [16] A. Knapitsch, E. Auffray, C.W. Fabjan, J.-L. Leclercq, X. Letartre, R. Mazurczyk, P. Lecoq, Results of photonic crystal enhanced light extraction on heavy inorganic scintillators, *IEEE Trans. Nucl. Sci.* 59 (2012) 2334–2339.
- [17] M. Kronberger, E. Auffray, P. Lecoq, Probing the concepts of photonic crystals on scintillating materials, *IEEE Trans. Nucl. Sci.* 55 (2008) 1102–1106.
- [18] Z. Zhu, S. Wu, C. Xue, J. Zhao, L. Wang, Y. Wu, B. Liu, C. Cheng, M. Gu, H. Chen, Enhanced light extraction of scintillator using large-area photonic crystal structures fabricated by soft-X-ray interference lithography, *Appl. Phys. Lett.* 106 (2015) 241901.
- [19] X. Chen, B. Liu, Q. Wu, Z. Zhu, J. Zhu, M. Gu, H. Chen, J. Liu, L. Chen, X. Ouyang, Enhanced light extraction of plastic scintillator using large-area photonic crystal structures fabricated by hot embossing, *Opt. Express* 26 (2018) 11438–11446.
- [20] Z. Zhu, B. Liu, C. Cheng, Y. Yi, W. Guo, S. Huang, H. Chen, M. Gu, C. Ni, X. Liu, Enhanced light extraction efficiency for glass scintillator coupled with two-dimensional photonic crystal structure, *Opt. Mater.* 35 (2013) 2343–2346.
- [21] Z. Zhu, B. Liu, C. Cheng, H. Chen, M. Gu, Y. Yi, R. Mao, Broadband light output enhancement for scintillator using whispering-gallery modes in nanospheres, *Phys. Status Solidi a* 211 (2014) 1583–1588.
- [22] J. Liu, B. Liu, Z. Zhu, L. Chen, J. Hu, M. Xu, C. Cheng, X. Ouyang, Z. Zhang, J. Ruan, Modified timing characteristic of a scintillation detection system with photonic crystal structures, *Opt. Lett.* 42 (2017) 987–990.
- [23] A. Knapitsch, E. Auffray, C.W. Fabjan, J.-L. Leclercq, X. Letartre, R. Mazurczyk, P. Lecoq, Effects of photonic crystals on the light output of heavy inorganic scintillators, *IEEE Trans. Nucl. Sci.* 60 (2013) 2322–2329.
- [24] Q. Wu, B. Liu, Z. Zhu, M. Gu, H. Chen, C. Xue, J. Zhao, Y. Wu, R. Tai, X. Ouyang, Directional emission of plastic luminescent films using photonic crystals fabricated by soft-X-ray interference lithography and reactive ion etching, *Sci. Rep.* 8 (2018) 1–8.
- [25] Z. Zhu, B. Liu, H. Zhang, W. Ren, C. Cheng, S. Wu, M. Gu, H. Chen, Improvement of light extraction of LYSO scintillator by using a combination of self-assembly of nanospheres and atomic layer deposition, *Opt. Express* 23 (2015) 7085–7093.
- [26] H.T. Miyazaki, H. Miyazaki, K. Ohtaka, T. Sato, Photonic band in two-dimensional lattices of micrometer-sized spheres mechanically arranged under a scanning electron microscope, *J. Appl. Phys.* 87 (2000) 7152–7158.
- [27] O.L. Hsu, C.W. Bates Jr., Luminescence phenomena in $CsI: Na$, *J. Lumin.* 11 (1975) 65–74.
- [28] O.L. Hsu, C.W. Bates Jr., Absorption and emission due to localized excitons in $CsI: Na$, *J. Lumin.* 15 (1977) 75–85.
- [29] O.L. Hsu, C.W. Bates Jr., Excitonic emission from $CsI (Na)$, *Phys. Rev. B* 15 (1977) 5821.
- [30] J. Liu, F. Liu, X. Ouyang, B. Liu, L. Chen, J. Ruan, Z. Zhang, J. Liu, The luminescence characteristics of $CsI (Na)$ crystal under α and X/γ excitation, *J. Appl. Phys.* 113 (2013) 023101.